Low-Aspect-Ratio Flat-Ship Theory

E. O. Tuck*
University of Adelaide, Adelaide, Australia

The integral equation, first obtained by H. Maruo, which determines the pressure distribution generating flow past a slender ip of vanishing draft, is studied further. New results obtained include predictions of singular centerplane effects of gravity for pointed bodies, a similarity solution for ships with cusped parabolic waterplanes, and some preliminary numerical solutions of the integral equation in the general case.

I. Introduction

THIS paper is an extension of a study by Maruo[1] on "ships of small draft," "flat ships," or "planing surfaces," all of which are equivalent descriptions. The small-draft assumption allows linearization of the free-surface boundary condition, as in the comparable case of thin ships, or ships of small beam.[2] However the present linearized problem is much harder to solve, since the generating singularity distribution (effectively a distribution of pressure points on the limiting waterplane) is not explicitly given in terms of hull shape, but requires solution of an integral equation. This problem is analogous to the lifting-surface problem of aerodynamics, whereas the thin-ship problem corresponds to the simpler thickness problem of aerodynamics.

Although this paper contains a brief reconsideration of the general flat-ship problem, to emphasize some aspects not discussed by Maruo, the paper is devoted mainly to the low-aspect-ratio limit. Thus the wetted length of the ship is supposed much greater than its beam, the latter having already been assumed much greater than the draft by the flat-ship requirement. The ship is therefore *not only flat, but also slender.*

An alternative derivation is given here of an integral equation equivalent to one obtained by Maruo, having as its unknown function a pressure distribution representing the ship. This integral equation is also obtainable from the high-Froude-number slender-body theory of Ogilvie,[3] by assuming that the ship is *not only slender, but also flat.*

Maruo's low-aspect-ratio flat-ship integral equation is formally valid only at moderately-high Froude numbers, specifically such that U^2B/gL^2 is a quantity of order unity, where U is ship speed, B its beam and L its length, and g is gravity. The equation reduces to that of low-aspect-ratio *wing* theory in aerodynamics as $g \to 0$. One approach to practical solution of any planing problem, whether or not the aspect ratio is low, is to expand in an asymptotic series for *very* high Froude number, commencing with the aerodynamic $g = 0$ limit as the leading term.[4] Maruo[1] obtains the first two terms in this series for the lift on a flat delta wing, and an alternative treatment of this class of expansion, for general hull shapes, is presented here. In particular, very strong effects of gravity near the center plane of pointed bodies are demonstrated.

At all Froude numbers, the low-aspect-ratio flat-ship integral equation possesses a "similarity" solution, such that the pressure distribution has the same shape at all stations. This linearized but gravity-dependent result should not be confused with the well-known conical similarity solution for nonlinear planing or water entry in the absence of gravity (Gilbarg,[5] p.360). In fact the present geometrical requirement is for a cusped parabolic waterplane shape but an arbitrary section shape, whereas the nonlinear zero-gravity solution requires a triangular plan form and section shape.

The low-aspect-ratio flat-ship integral equation is amendable to direct computation, and we present here some preliminary examples of its numerical solution. Much more work needs to be done to derive efficient procedures, and the present computer program can only be considered as a crude first attempt. However, the results are of considerable interest, indicating rather dramatic gravity effects especially near the center plane, as predicted analytically, and confirming Maruo's[1] estimate of the lift coefficient of a delta wing at sufficiently high Froude number.

II. The General Flat Ship Problem

A rather unconventional co-ordinate system, (x, y, s), is used as in Tuck and von Kerczek[6] (Fig.1). The ship is supposed fixed with its bow at $s=0$ and stern at $s=L$ in a stream U. Thus the total flowfield velocity is

$$q = \nabla (Us + \phi) \tag{1}$$

where ϕ is the perturbation velocity potential.

The body equation is

$$y = \eta(x,s) \tag{2}$$

where η is generally expected to be negative, "$-\eta$" being the depth of the buttock line x=constant at station s. Equation

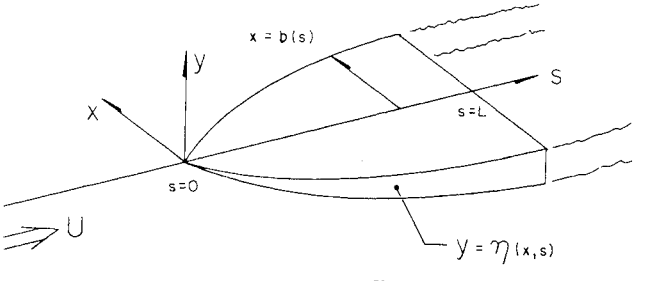

Fig. 1 Sketch of coordinate system.

Received September 27, 1974; This research was carried out under the Naval Ship Systems Command, General Hydromechanics Research Program, Subproject SR 009 01 01, administered by the Naval Ship Research and Development Center, Contract N00014-67-A-0181-0052.

Index categories: Hydrodynamics; Marine Hydrodynamics, Vessel and Control Surface.

*Professor of Applied Mathematics; formerly Visiting Professor of Fluid Mechanics, Department of Naval Architecture and Marine Engineering, University of Michigan, Ann Arbor, Mich., Academic Year 1972-1973.

(2) is supposed to hold for

$$|x|<b(s) \tag{3}$$

where $b(s)$ is the half-waterplane width at station s. For $|x|>b$ we may suppose that Eq. (2) defines the water surface elevation. The hull boundary condition is

$$\phi_y=(U+\phi_s)\eta_s+\phi_x\eta_x \tag{4}$$

to be applied on the exact hull surface $y=\eta$.

We first make the small-draft approximation, introducing a small parameter α measuring the draft/length ratio. Keeping only leading order terms with respect to α, the boundary condition Eq. (4) reduces to

$$\phi_y=U\eta_s \qquad \text{on } y=0 \tag{5}$$

It is important to note that the small-α approximation is a regular one, as distinct from the (potentially) singular perturbation represented by the small -ϵ slenderness approximation to be applied next, where ϵ measures the beam/length ratio. It shall be assumed that $\alpha<<\epsilon$, so that Eq. (5) may be taken to hold quite accurately when the small ϵ approximation is made.†

The boundary condition, Eq. (4), also correctly gives the exact kinematic condition on the unknown free surface $y=\eta$ for $|x|>b$. This has to be supplemented by the dynamic condition

$$P/\rho+U\phi_s+\tfrac{1}{2}|\nabla\phi|^2+g\eta=0 \tag{6}$$

if the excess of pressure over atmospheric at the free surface is P; usually $P=0$. Again, the small-draft approximation enables linearization not only of Eq. (4) but also of Eq. (6) to give on $y=0$.

$$P/\rho+U\phi_s+g\eta=0 \tag{7}$$

which combines with Eq. (5) to give the linearized free-surface condition

$$g\phi_y+U^2\phi_{ss}=-(U/\rho)P_s \tag{8}$$

If $P=0$, this reduces to the usual equation

$$g\phi_y+U^2\phi_{ss}=0 \tag{9}$$

However, we shall generate solutions by means of pressure distributions P, the velocity potentials then satisfying Eq. (8) whenever $P\neq 0$. Note that Eq. (9) results from the small-α approximation, and that alone; when we subsequently take ϵ as small, Eq. (9) may be considered as exact.

The general flat-ship problem, with ϵ not necessarily small, is that of solving the full Laplace equation

$$\phi_{xx}+\phi_{yy}+\phi_{ss}=0 \tag{10}$$

in the space $y<0$, subject to the hull condition, [Eq. (5)] on the wetted portion W: $|x|<b(s)$, of the plane $y=0$ occupied by the projection of the hull, and the linearized free-surface condition Eq. (9) on the portion $|x|>b(s)$. In addition we expect to require some kind of radiation condition at infinity, and a Kutta-type condition that the pressure reduces to atmospheric pressure at any sharp trailing edge in order that the free surface leave such an edge smoothly.

This problem can be converted into an integral equation, which is the finite-Froude-number analogue of the lifting-surface integral equation of aerodynamics. Maruo[1] gives one method for accomplishing this; perhaps more directly we may set ourselves the task of finding an unknown surface pressure distribution $P(x,s)$ which generates the free-surface displacement $\eta(x,s)$. The corresponding integral connection‡ between P and η may be obtained from well-known formulas, e.g., Wehausen and Laitone,[22] p.598. For example

$$\pi^2\rho U^2\eta_s(x,s)= -Im\iint_W d\xi\, d\sigma\, P(\xi,\sigma)\int_0^{\pi/2} d\theta\, \sec\theta \times \int_0^\infty dk\, \frac{k^2 e^{-ik(s-\sigma)\cos\theta}\cos(k(x-\xi)\sin\theta)}{k-g/U^2\sec^2\theta} \tag{11}$$

where the path of k-integration goes above the pole.

We shall not attempt to solve this integral equation here, since our concern is with the low-aspect-ratio case. However, several questions are worth noting. Maruo[1] states that "the kernel of the integral equation is complicated enough to frustrate any attempt at solving it." This view is perhaps a little too pessimistic. The kernel is simply the complete solution for a traveling three-dimensional pressure point, and a number of similar computations have been carried out on an ad hoc basis recently, e.g., Monacella and Newman,[9] Gadd,[10] and van Oortmerssen.[11] Of course there is more to the solution of the integral equation than just evaluating its kernel; however, direct numerical attack on this general flat-ship problem would seem worthwhile, and some effort is being put into this.[12]

The role of the Kutta, or constant-pressure, condition at the trailing edge is worth comment. There is a degree of non-uniqueness about the integral equation (11); the homogeneous equation with $\eta_s=0$ has a nontrivial set of solutions. This is illuminated by performing an indefinite s-integration of Eq. (11), introducing thereby an arbitrary function of x on the left-hand side, say $C(x)$. The resulting integrated operator permits a unique solution, the non-uniqueness being now absorbed into $C(x)$. This unknown function must somehow be determined by the requirement that $P(x,s)$ vanishes at the trailing edge. Physically, this indeterminateness is equivalent to a degree of indeterminateness about the vertical location of the hull, and indeed at infinite aspect ratio, $\partial/\partial x\equiv 0$, C is a constant, reflecting bodily upward or downward shift of the original given foil relative to the undisturbed free surface at infinity. A practically more useful, but mathematically more difficult, procedure is to set $C\equiv 0$, but instead allow W, or the wetted length at each x, to be indeterminate.

The zero- and infinite-Froude-number limits of Eq. (11) are of interest. In the zero-Froude-number case we obtain simply

$$P(x,s)=-\rho g\eta(x,s) \tag{12}$$

i.e., the appropriate pressure is hydrostatic. This is the apparent basis for the original flat-ship formula of Hogner (see Havelock[13]), which is however inconsistent, if used in a wave-resistance calculation at finite Froude number. At infinite Froude number, the integral equation reduces exactly to that of aerodynamic lifting-surface theory, so that the ship is equivalent to a lifting wing with camber surface $y=\eta(x,s)$. The role played by the Kutta condition however, is quite different, as noted above.

The analogy between the flat-ship theory and lifting-surface theory, which becomes an exact equivalence at $g=0$, illustrates a disturbing feature of the low-aspect-ratio flat-ship theory, namely that we shall not in general be able to

†Note that, according to Acosta and DeLong,[7] the infinite-Froude-number slender-planing-surface analysis of Tulin[7] is valid in the opposite limit $\epsilon<<\alpha$.

‡An interesting physical interpretation of this connection is the statement: "Every planing surface is hydrodynamically equivalent to some hovercraft." The equivalent hovercraft does not, of course, have a uniform base pressure.

satisfy the Kutta condition once the low-aspect-ratio approximation has been made. That is, the pressure predicted by the low-aspect-ratio theory at the edge of the transom stern will not in general be atmospheric. This would be a most unfortunate conclusion, were it not for the fact that low-aspect-ratio wing theory also suffers from this deficiency, yet nevertheless has proved useful. What presumably happens is that in a small neighborhood of the trailing edge there is a rapid change of pressure back to atmospheric. The hope is that this occurs over a dynamically-insignificant portion of the total hull and has no significant upstream effect. Some work has been done[14] on the corresponding aerodynamic problem.

III. Derivation of the Low-Aspect-Ratio Flat-Ship Integral Equation

We now assume that the hull has a low aspect ratio, i.e., that it is slender, in the sense that its beam B is much smaller than its length L, say $B=0(\epsilon)L$. Note however that there is a definite heirachy of smallness in this problem; thus "Draft $\ll$ Beam $\ll$ Length." The case when the draft and beam are comparable gives ordinary slender-ship theory, as in Tuck[15] for low-to-moderate Froude numbers, and Ogilvie[3] for moderate-to-high Froude numbers.

In the present case we are going to treat moderate-to-high Froude numbers, such that

$$\nu = gL^2/U^2B \tag{13}$$

is of order unity. This means that the conventional length-based Froude number is large, specifically

$$F = U/(gL)^{1/2} = 0[(L/B)^{1/2}] = 0(\epsilon^{-1/2}) \tag{14}$$

This is the regime treated by Ogilvie[3] and by Maruo.[1] In fact the appropriate integral equation can be obtained by specializing Ogilvie's inner problem, for the case of small draft/beam ratio. Ogilvie's general problem requires solution of a nonlinear two-dimensional free-surface problem in each cross-section. The small-draft approximation linearizes this problem and can lead to the same integral equation as is obtained by the reverse procedure, i.e., of "small α, then small ϵ", rather than "small ϵ, then small α."

Since the body is slender, the problem becomes two-dimensional in the (x,y) cross-flow plane; i.e., dropping ϕ_{ss} from the Laplace equation (10) gives

$$\phi_{xx} + \phi_{yy} = 0 \tag{15}$$

In the Froude-number range in which $\nu = 0(1)$ it is clear that both terms in the free-surface condition of Eq. (9) must be retained, since $\partial/\partial s = 0(L^{-1})$ and $\partial/\partial y = 0(B^{-1})$.

If we temporarily define a "pseudo-time" co-ordinate t by the equation

$$s = Ut \tag{16}$$

the free-surface condition Eq. (9) becomes

$$g\phi_y + \phi_{tt} = 0 \tag{17}$$

which is identical to the usual *unsteady* linearized free-surface condition for water waves. Thus, since ϕ now satisifies Eq. (15), not Eq. (10), we can use any solution for unsteady two-dimensional linearized water waves, replacing t by s/U.

The solution of most direct use is again that of a pressure distribution $P(x,s)$ over the free surface. This is now to be interpreted as "time" – varying pressure distribution imposed on a segment $|x| < b(s)$ of the axis $y=0$, whose width $2b(s)$ also varies with "time."

The solution is given by Wehausen and Laitone[22] p.615. It is convenient to write it in terms, not of the velocity potential $\phi(x,y,s)$, but rather of its conjugate, the stream function $\psi(x,y,s)$. In fact, since from now on we shall be concerned only with $y=0$, for brevity we write $\psi(x,s)$ for $\psi(x,0,s)$. Thus

$$\rho U\psi(x,s) = \int_0^s d\sigma \int_{-b(\sigma)}^{b(\sigma)} d\xi\ P(\xi,\sigma)\ K(x-\xi, s-\sigma) \tag{18}$$

where

$$K(x,s) = \pi^{-1} \int_0^\infty d\lambda\ \sin\lambda x\ \cos[(g\lambda/U^2)^{1/2} s] \tag{19}$$

$$= (\pi x)^{-1} F'(\omega) \tag{20}$$

with

$$\omega^2 = \frac{gs^2}{4U^2|x|} \tag{21}$$

and

$$F'(\omega) = 1 + 2\omega \int_0^\omega d\zeta\ \sin(\zeta^2 - \omega^2)$$

$$= \frac{d}{d\omega} \int_0^\omega d\zeta\ \cos(\zeta^2 - \omega^2) \tag{22}$$

The function $F'(\omega)$ can be expressed in terms of Fresnel integrals, e.g.

$$F'(\omega) = 1 + 2\omega\sqrt{\pi/2}\ [\cos\omega^2\ S(\sqrt{\pi/2}\ \omega) - \sin\omega^2\ C(\sqrt{\pi/2}\ \omega)] \tag{23}$$

$$= 1 + 2\omega\sqrt{\pi/2}\ \left[\frac{\cos\omega^2}{2} - \frac{\sin\omega^2}{2} - f(\sqrt{2/\pi}\ \omega)\right] \tag{24}$$

where S, C are Fresnel integrals, and $f(\zeta)$ is an auxiliary function.[16] The function $F'(\omega)$ has convenient series and asymptotic expansion, respectively,

$$F'(\omega) = 1 + \sum_{m=1}^{\infty} \frac{(-4\omega^4)^m}{1\cdot 3\cdot 5\cdot \ldots (4m-3)\cdot(4m-1)} \tag{25}$$

which can be used for small ω, and

$$F'(\omega) = (\pi/2)^{1/2}\omega(\cos\omega^2 - \sin\omega^2) - \sum_{m=1}^{m_\infty} \frac{1\cdot 3\cdot 5\cdot \ldots (4m-3)\cdot(4m-1)}{(-4\omega^4)^m} \tag{26}$$

which can be used for large ω, and a suitable stopping point m_∞.

The kernel K and function $F'(\omega)$ occur also in classical Cauchy-Poisson problems[17] and the physical description of the spreading waves produced is well-known. Indeed one can view the representation Eq. (18) as physically resulting from a "time" history of pressure pulses, the pulse $P(x,s)$ at "time" $\sigma = s$ being applied in order to cancel out instantaneously the spreading waves produced at earlier "times" $\sigma < s$. Our aim is to choose $P(x,s)$ so that the stream function which is left over after this cancellation correctly satisfies the hull boundary condition. Somewhat similar ideas were used by Cummins.[18]

The boundary condition, Eq. (5), is written in terms of ϕ. However, using the Cauchy-Riemann equation $\phi_y = -\psi_x$, we have

$$\psi(x,s) = -U \int_0^x \eta_s(\xi,s)\ d\xi \tag{27}$$

Note that we have used the natural antisymmetry condition $\psi=0$ at $x=0$. Thus once the hull shape $\eta(x,s)$ is given, $\psi(x,s)$ may be treated as a known function, and Eq. (18) then represents an integral equation to determine the unknown pressure $P(x,s)$. For example, if the "ship" is a flat plate[§] at an angle of attack α then

$$\eta(x,s) = -\alpha s \tag{28}$$

and we have immediately

$$\psi(x,s) = U\alpha x \tag{29}$$

The analytical character of the integral equation (18) is of some interest. The equation is of Fredholm character with respect to the (space-like) variable x with dummy ξ, and of Volterra character with respect to the (time-like) variable s with dummy σ (Tricomi.[19]). This means physically that information at *all* values of ξ is needed to determine the solution at *any* x, whereas only information at further *forward* stations $\sigma<s$ is needed to determine the solution at a particular station s. We may hope to solve the equation in the s-dimension by a time-stepping or marching process, proceeding systematically from bow to stern, as in an *initial-value* problem for a differential equation. But at each station s we must expect to solve the Fredholm integral equation with respect to x in a manner more like a *boundary-value problem* for a differential equation.

Furthermore, the Fredholm equation in the x direction is *singular*. This is most apparent at $g=0$, where $\omega=0$ and $F'(\omega)=F'(0)=1$. Thus at $g=0$, $K(x-\xi,s-\sigma)=1/\pi(x-\xi)$ and the ξ-integration is to be interpreted in the sense of Cauchy. In fact for any $g\neq 0$ and $\sigma\neq s$ the singularity is in a sense *worse* than the simple Cauchy pole, for as $\omega\to\infty$ we have from Eq. (26)

$$F'(\omega) \to (\pi/2)^{1/2}\omega(\cos\omega^2 - \sin\omega^2) \tag{30}$$

Thus as $\xi \uparrow x$,

$$K(x-\xi,s-\sigma) \to (g/8\pi U^2)^{1/2}(s-\sigma)(x-\xi)^{-3/2} \times \cos\left[\frac{g(s-\sigma)^2}{4U^2(x-\xi)} + \frac{\pi}{4}\right] \tag{31}$$

Hence if $\sigma\neq s$, the kernel function behaves like a $-3/2$ power multiplied by a rapidly oscillating function, as $\xi\to x$. This behavior may be expected to cause some degree of numerical difficulty, and does.

Instead of tackling the integral equation for the pressure P itself directly, it is somewhat more convenient to work in terms of a function Q whose s derivative is P, namely

$$Q(x,s) = \int_{-\infty}^{s} P(x,\sigma)\, d\sigma \tag{32}$$

Although the lower limit of Eq. (32) is written as "$-\infty$," it may equally well be replaced by zero, or in fact by $s_0(x)$, where $s_0(x)$ is the station s at which $x=b(s)$; i.e., the function $s_0(x)$ is the mathematical inverse of the function $b(s)$. This is because $P\equiv 0$ outside the hull projection on the plane $y=0$.

The function $Q(x,s)$ is of course the loading on a unit-width strip of the hull at offset x, extending from the leading edge to station s. Hence, for example, the total lift force F_y in the y direction is obtained in terms of the values of Q at the trailing edge $s=L$, namely

$$F_y = \int_{-b(L)}^{b(L)} Q(x,L)\, dx \tag{33}$$

More-complicated formulas involving Q at all stations s apply to the pitching moment and the drar. At infinite Froude number, Q is proportional to the velocity potential ϕ; specifically

$$Q = -\rho U\phi \tag{34}$$

However, as is clear from the boundary condition (8), no such identification is possible if $g\neq 0$.

On substituting $P(\xi,\sigma)=Q_\sigma(\xi,\sigma)$ in Eq. (18) and integrating by parts with respect to σ, we have

$$\begin{aligned}\rho U\psi(x,s) &= \left[\int_{-b(\sigma)}^{b(\sigma)} d\xi\, Q(\xi,\sigma)\, K(x-\xi,s-\sigma)\right]_{\sigma=0}^{\sigma=s} \\ &\quad - \int_0^s d\sigma \int_{-b(\sigma)}^{b(\sigma)} d\xi\, Q(\xi,\sigma)\, K_\sigma(x-\xi,s-\sigma) \\ &= \int_{-b(s)}^{b(s)} d\xi\, Q(\xi,s)\, K(x-\xi,0) \\ &\quad - \int_0^s d\sigma \int_{-b(\sigma)}^{b(\sigma)} d\xi\, Q(\xi,\sigma)\, K_\sigma(x-\xi,s-\sigma)\end{aligned} \tag{35}$$

using $Q=0$ at $x=b(s)$.

The first term of Eq. (35) involves $K(x-\xi,0)$ which is simply $1/\pi(x-\xi)$. Thus this term must be interpreted in the sense of Cauchy, and takes the form of a finite Hilbert transform[19] which we write symbolically as

$$\mathcal{H}_{b(s)}\, Q(x,s) \equiv \frac{1}{\pi}\int_{-b(s)}^{b(s)} \frac{d\xi\, Q(\xi,s)}{x-\xi} \tag{36}$$

Thus Eq. (35) becomes

$$\rho U\psi(x,s\ 3\mathcal{H}_{b(s)}\, Q(x,s) - \int_0^s d\sigma \int_{-b(\sigma)}^{b(\sigma)} d\xi\, Q(\xi,\sigma)\, K_\sigma(x-\xi,s-\sigma) \tag{37}$$

This equation is the principal integral equation we shall attempt to solve. The kernel K_σ may, after some manipulation, be written in the form

$$K_\sigma(x-\xi,s-\sigma) = \frac{2}{\pi(s-\sigma)}\frac{\partial}{\partial\xi}F'(\omega) \tag{38}$$

where

$$\omega^2 = \frac{g(s-\sigma)^2}{4U^2|x-\xi|} \tag{39}$$

Equation (37) agrees with the result of integrating Maruo's[1] Eq. (57) with respect to our ξ, from $\xi=0$ to $\xi=x$. Table 1 shows the equivalence of the various symbols used. Note that the function $F(x,y)$ used by Maruo[1] in his Eq. (58) et seq. was never defined, but is related to our $K(x,s)$. Maruo's Eq. (56), when similarly integrated with respect to our ξ, also agrees with our Eq. (18).

IV. High-Froude-Number Limit

The limit $g\to 0$ may be carried out on either Eq. (18) or Eq. (37). In any case, if $g=0$ the kernel $K(x-\xi,s-\sigma)$

§Or, in fact, any hull differing from that given by Eq. (28) by addition of a function of x alone; for example, a triangular section with a constant deadrise angle qualifies. Only the longitudinal slope η_s is hydrodynamically significant. Problems regarding the uniqueness of the section shapes for a given planform W are still under investigation. In the meantime, the term "flat plate," where used in the present paper, should be interpreted as implying a body with a constant longitudinal slope, but not necessarily a rectangular section shape.

Table 1 Equivalence of symbols

This paper	Maruo[1]
s,σ	$x+\mathfrak{L},x'+\mathfrak{L}$
x,ξ	y,y'
y	z
$\eta(x,s)$	$f(x,y)$
$P(x,s)$	$\rho U\gamma(x,y)$
$Q(x,s)$	$\rho U^2 g(x,y)$
$-\eta_s(x,s)$	$\omega(x,y)$
$\psi(x,s)$	$\int_0^y \omega(x,y')\,dy'$
$b(s)$	$bs(x/\mathfrak{L})$
$B=2b(L)$	$2b$
L	$2\mathfrak{L}$
F	$(2\chi_0)^{-1/2}$
ν	$2\chi_0\mathfrak{L}/b$
F_y	L

$=1/\pi(x-\xi)$ is independent of s and σ. Hence in Eq. (37), $K_\sigma=0$ and the intergral equation reduces to

$$\mathcal{H}_b Q(x,s)=\rho U\psi(x,s) \tag{40}$$

There is now neither upstream nor *downstream* influence of the loading at one station on another, and the problem is solved immediately by inversion of the finite Hilbert transform, using the inverse Hilbert transform operator defined symbolically by[19]

$$\mathcal{H}_b^{-1}=-(b^2-x^2)^{1/2}\mathcal{H}_b(b^2-x^2)^{-1/2} \tag{41}$$

Thus

$$\begin{aligned}Q(x,s)&=-\rho U(b^2-x^2)^{1/2}\mathcal{H}_b(b^2-x^2)^{-1/2}\psi(x,s)\\&=-\frac{\rho U[b^2(s)-x^2]^{1/2}}{\pi}\\&\quad\times\int_{-b(s)}^{b(s)}\frac{d\xi\ \psi(\xi,s)}{[b^2(s)-\xi^2]^{1/2}(x-\xi)}\end{aligned} \tag{42}$$

Normally the inverse operator, $\mathcal{H}_b^{-1}$ is not uniquely defined, and to any solution such as Eq. (42) we must add a multiple of the function $(b^2-x^2)^{-1/2}$ whose Hilbert transform vanishes.[19] However, we can exclude this possibility in the present case, since this would generate velocity and pressure distributions with inverse 3/2 power singularities at the leading edge $x=b(s)$. In order to retain only integrable (inverse square root) pressure singularities, we must require a square-root zero in Q, leading to the solution in Eq. (42).

Since Q is proportional to the velocity potential when $g=0$, Eq. (42) could also have been obtained directly from the boundary-value problem with $\phi=0$ as the free surface condition, and simply expresses the fact that conjugate harmonic functions such as ϕ and ψ are Hilbert transforms of each other on the x-axis. This solution is of course well known in aerodynamic low-aspect-ratio wing theory.[20] The solution for a flat plate is simply

$$Q(x,s)=\rho U^2\alpha[b^2(s)-x^2]^{1/2} \tag{43}$$

the usual "elliptic loading distribution."

We are here interested rather in the first correction term to Q, resulting from finite-Froude-number effects. That is, we seek an asymptotic expansion for small g (or more correctly for small values of the appropriate normalized gravity parameter $\nu=gL^2/U^2B$), which begins with a term $Q=Q^\infty$ given by Eq. (42). Maruo[1] has performed such an analysis on the lift coefficient in a special case and has proved that the first correction to the infinite-Froude-number lift is a factor of order ν, which means that the asymptotic expansion at least begins like a Taylor series with respect to ν.

A logical procedure for constructing this expansion is by successive approximation; i.e., since Eq. (42) resulted from dropping the last term of Eq. (37) entirely, the first correction to Eq. (42) is obtained by substitution of Q^∞ into this particular term. Thus if

$$Q=Q^\infty+Q^1 \tag{44}$$

where $Q^1\to 0$ as g or $\nu\to 0$, we have

$$\mathcal{H}_{b(s)}Q^1=\int_0^s d\sigma\int_{-b(\sigma)}^{b(\sigma)}d\xi\ Q^\infty(\xi,\sigma)K_\sigma(x-\xi,s-\sigma) \tag{45}$$

While Eq. (45) may be a useful formula as it stands, we can simplify further, since K itself still depends on gravity g. But if, for example, we were to use the (truncated) series of Eq. (25) to estimate K_σ for small g, we should only obtain terms of $0(g^2)$, not $0(g)$ as expected from Maruo's analysis. Furthermore, the resulting integrals would diverge because of a nonintegrable singularity at $\xi=x$. The highly oscillatory behavior of the kernel near $\xi=x$, as indicated by Eq. (31), suggests that the limit $g\to 0$ needs special treatment, and it is clear by analogy with the method of stationary phase that only the neighborhood of $\xi=x$ contributes significantly to the integral equation (45), to leading order.

Thus we expand Q^∞ in a Taylor series about $\xi=x$, giving

$$\mathcal{H}_bQ^1=\int_0^s d\sigma\ \times\int_{\substack{\text{(nbhd}\\ \text{of }x)}}d\xi\ [Q^\infty(x,\sigma)+(\xi-x)Q_x^\infty(x,\sigma)+\ldots]K_\sigma \tag{46}$$

However, ξ can only take values near to x for $s_0(x)<\sigma<s$ where $s_0(x)$ is defined below Eq. (32). Further, in view of Eq. (38), the term of Eq. (46) in $Q^\infty(x,\sigma)$ integrates to zero, and we are left with

$$\begin{aligned}\mathcal{H}_bQ^1&=-\frac{2}{\pi}\int_{s_0(x)}^s d\sigma\frac{Q_x^\infty(x,\sigma)}{s-\sigma}\\&\quad\times\int_{x-\infty}^{x+\infty}d\xi(\xi-x)\frac{\partial}{\partial\xi}F'(\omega)\end{aligned} \tag{47}$$

$$\begin{aligned}&=+\frac{4}{\pi}\int_{s_0(x)}^s d\sigma\frac{Q_x^\infty(x,\sigma)}{s-\sigma}\\&\quad\times\int_0^\infty d\chi\,[F'(\omega)-1]\end{aligned} \tag{48}$$

where $\chi=|\xi-x|$ and $\omega^2=g(s-\sigma)^2/4U^2\chi$. On changing the variable of integration from χ to ω, we have

$$\begin{aligned}\mathcal{H}_bQ^1&=\frac{2g}{\pi U^2}\int_{s_0(x)}^s d\sigma(s-\sigma)\,Q_x^\infty(x,\sigma)\\&\quad\times\int_0^\infty\frac{F'(\omega)-1}{\omega^3}d\omega\end{aligned} \tag{49}$$

The last integral with respect to ω is a pure constant, taking the value "-2π." Thus, finally,

$$\mathcal{H}_{b(s)}Q^1(x,s)=-\frac{4g}{U^2}\int_{s_0(x)}^s d\sigma(s-\sigma)Q_x^\infty(x,\sigma) \tag{50}$$

The procedure for computing the leading-order gravity effects on the flow (and in particular on the pressure distribution) is thus to compute first the infinite-Froude-number solution $Q^{\infty}(x,s)$ by Eq. (42), substitute into Eq. (50), then take a further inverse Hilbert transform to find $Q^1(x,s)$. Except in very special cases this procedure may be nearly as difficult as direct numerical solution of the integral equation (37). However, we note that the leading-order dependence on gravity g is linear, as in Maruo's estimate[1] for the lift coefficient of a flat delta wing.

In the special case of the flat plate we may proceed a little further. Thus on use of Eq. (43) for Q^{∞} in Eq. (50), we have

$$\mathcal{H}_b Q^1 = 4g\rho\alpha x \int_{s_0(x)}^{s} \frac{d\sigma(s-\sigma)}{[b^2(\sigma)-x^2]^{1/2}} \tag{51}$$

It should be observed that the denominator vanishes at the lower limit $\sigma = s_0(x)$ of the σ integration. In the further special case of a triangular waterplane

$$b(s) = \lambda s \tag{52}$$

we can integrate Eq. (51) explicitly to give

$$\mathcal{H}_b Q^1 = 4g\rho(\alpha/\lambda)x\{s \log[s + (s^2 - (x^2/\lambda^2))^{1/2}]$$
$$- \tfrac{1}{2}[s^2 - (x^2/\lambda^2)]^{1/2} - s\log(|x|/\lambda)\} \tag{53}$$

Although no doubt the inverse Hilbert transform could now be obtained to generate Maruo's solution, our purpose here is rather to observe the remarkable introduction of singular behavior along the center line $x=0$, as evidenced by the term of Eq. (53) in "$\log|x|$." This behavior is characteristic of pointed flat plates. For example, if we consider the more general class of waterplanes whose behavior near the bow is of the form

$$b(s) = \lambda s^n \tag{54}$$

for some positive exponent n, then the behavior of the intergral equation (51) as $x \to 0$ is of the form of an analytic function of x, plus a contribution of the order of $s \cdot x^{1/n}$, $n \neq 1$, or $s \cdot x \log x$, $n=1$. Thus for all $n \geq 1$, the slope of the graph of the function $\mathcal{H}_b Q^1$ against x is infinite at $x=0$. The function $\mathcal{H}_b Q^1$ is, of course, an *odd* function of x.

The corresponding result for Q^1 itself is that Q^1 behaves like an analytic *even* function of x, plus a contribution of the order of $s \cdot |x|^{1/n}$ for all $n \neq 1/2$, and $s \cdot x^2 \log|x|$ for $n = 1/2$. Specifically, we have

$$Q^1(x,s) = Q^1(0,s) + \begin{cases} 0(x^2), & 0 < n < \tfrac{1}{2} \\ s \cdot 0(x^2 \log|x|), & n = \tfrac{1}{2} \\ s \cdot 0(|x|^{1/n}), & n > \tfrac{1}{2} \end{cases} \tag{55}$$

It should be noted that since $P = Q_s$, and the singular terms of Eq. (55) are linear in s, Eq. (55) indicates that the pressure distribution P itself has the same singular structure, with the strength of the singularities invariant along the length of the ship.

Thus for $0 < n < 1/2$, the pressure is well behaved, for $n = 1/2$ (blunt parabolic waterplane) the lateral pressure gradient vanishes at $x=0$ but the lateral curvature of the graph of pressure against x is infinite, and similarly for $1/2 < n < 1$. For $n=1$ (triangular waterplane) the lateral pressure gradient is discontinuous but finite at $x=0$ while for all $n > 1$ the lateral pressure gradient is infinite at $x=0$. That is, there is a very sharp but finite-magnitude pressure peak along the center line of any sharply-pointed flat plate.

The above result is of course essentially a gravitational effect, and stands in sharp contrast to the smooth behavior of the elliptic loading Eq. (43) in the gravity-free case. The singularity is presumably due to the profound effect of the diverging waves generated at the extreme bow, whose wave length tends to zero along the track of the bow, irrespective of Froude number.[21] Although the above analytic conclusions were obtained from a high-Froude-number expansion, it is probable that the essential character of the singularity is the same at all Froude numbers, and the numerical solution of Sec. VII tends to verify this.

V. A Similarity Solution

This section presents a solution $P(x,s)$ of the integral equation (18) which has the same basic shape at all stations s. That is, the pressure distribution at any one station s is obtained from that at any other station by a simple scaling of P and x. The x-wise scale is obviously $b(s)$, and it is easy to see that the only possible multiplicative scale on P is some power of s. Thus we seek a solution of the form

$$P(x,s) = s^{\gamma} \boldsymbol{P}[x/b(s)] \tag{56}$$

for some constant γ and some function $\boldsymbol{P}(x)$ of a single variable $\boldsymbol{x}$.

Of course we have no guarantee that such a solution ever exists, and in particular could not expect it to exist without some special restriction on $b(s)$. In fact, we shall now show that Eq. (56) is a valid solution if and only if the waterplane consists of cusped parabolas, i.e., if

$$b(s) = \lambda s^2 \tag{57}$$

for some constant $\lambda = B/2L^2$. The body shape $\eta(x,s)$ and thus the stream function $\psi(x,s)$ will also possess a similarity character, and we shall verify that, for example,

$$\psi(x,s) = s^{\gamma+1} \boldsymbol{\psi}[x/b(s)] \tag{58}$$

The foregoing are the most general assumptions which permit a similarity solution. To verify that they are consistent, and to find the equation satisfied by $\boldsymbol{P}(x)$, we substitute Eqs. (56) and (58) into the integral equation (18).

Thus we have

$$\rho U s^{\gamma+1} \boldsymbol{\psi} \frac{x}{b(s)} = \int_0^s d\sigma\, \sigma^{\gamma} b(\sigma) \times$$
$$\int_{-1}^{1} d\xi\, \boldsymbol{P}(\xi)\, K(x - \xi b(\sigma), s - \sigma) \tag{59}$$

on substituting $\xi = \xi b(\sigma)$. Putting $x = \boldsymbol{x} b(s)$, and using the form [Eq.(20)] of K gives

$$\rho U s^{\gamma+1} \boldsymbol{\psi}(\boldsymbol{x}) = \frac{1}{\pi} \int_0^s d\sigma\, \sigma^{\gamma} \int_{-1}^{1} \frac{d\xi\, \boldsymbol{P}(\xi)}{\mu \boldsymbol{x} - \xi} F'(\omega) \tag{60}$$

where

$$\mu = b(s)/b(\sigma) \tag{61}$$

and

$$\omega^2 = \frac{g(s-\sigma)^2/b(\sigma)}{4U^2|\mu x - \xi|} \tag{62}$$

If we put $\sigma = st$ in Eq.(60)

$$\rho U \boldsymbol{\psi}(\boldsymbol{x}) = \frac{1}{\pi} \int_{-1}^{1} d\xi\, \boldsymbol{P}(\xi) \int_0^1 \frac{dt\, t^{\gamma} F'(\omega)}{\mu \boldsymbol{x} - \xi} \tag{63}$$

where now

$$\mu = b(s)/b(st) \tag{64}$$

and

$$\omega^2 = \frac{gs^2(1-t)^2/b(st)}{4U^2|\mu x-\xi|} \tag{65}$$

So far, the assumption (57) was not made. In order that the original assumption (56) be valid it is necessary that Eq. (63) represent an integral equation for $P(x)$; i.e., that it be independent of the station coordinate s. The parameter μ is independent of s if and only if b is proportional to some power of s, while the parameter ω is independent of s if and only if that power is exactly 2. Thus if Eq. (57) is satisfied,

$$\mu = t^{-2} \tag{66}$$

and

$$\omega^2 = \frac{g(1-t)^2}{4\lambda U^2|x-t^2\xi|} = \tfrac{1}{2}\nu\frac{(1-t)^2}{|x-t^2\xi|} \tag{67}$$

Thus, finally, the integral equation for $P(x)$ can be written

$$\rho U\psi(x) = \int_{-1}^{1} d\xi\, P(\xi)\, K(x,\xi) \tag{68}$$

where

$$K(x,\xi) = \frac{1}{\pi}\int_0^1 \frac{dt\, t^{\gamma+2}}{x-\xi t^2}\, F'(\omega) \tag{69}$$

with ω determined by Eq.(67)

The task of solving the one-dimensional integral equation (68) would appear to be considerably simpler than that of solving the general two-dimensional equation (18). However, the kernel $\mathbf{K}$ is obviously extremely complicated, and highly singular as $\xi \to x$. Hence numerical similarity solutions have so far been obtained only indirectly, via the general equation, and will be presented in Sec. VII.

The quantity $Q(x,s)$ whose s derivative is P also obeys a similarity law, of the form

$$Q(x,s) = s^{\gamma+1} Q[x/b(s)] \tag{70}$$

On differentiation with respect to s, we establish the connection

$$P(x) = (\gamma+1)\, Q(x) - 2x\, Q'(x) \tag{71}$$

between the similarity profiles of P and Q. An integral equation for Q may also be obtained by substitution of Eq. (70) into Eq. (37), namely

$$\rho U\psi(x) = \mathcal{K}_1 Q(x) + \int_{-1}^{1} d\xi\, Q(\xi)\frac{\partial}{\partial\xi} K_1(x,\xi) \tag{72}$$

where

$$K_1(x,\xi) = \frac{2}{\pi}\int_0^1 \frac{dt\, t^{\gamma+1}}{1-t}[F'(\omega)-1] \tag{73}$$

ω being given by Eq. (67) again.

The allowed shapes of the hull are of interest. Clearly we are allowed only the very specific cusped waterline prescribed by Eq. (57). However, considerably greater latitude is allowed in the shape of the cross-sections and some latitude is allowed in the longitudinal profile. Thus it is clear that the hull function η also has a similarity character, with

$$\eta(x,s) = s^{\gamma}\eta[x/b(s)] \tag{74}$$

The arbitrary exponent γ therefore characterizes the longitudinal profile or keel line, which is straight if $\gamma=1$, blunt if $\gamma<1$ and cusped if $\gamma>1$.[¶]

The case of a flat plate is included, with $\gamma=1$ and $\eta(x) = -\alpha =$ constant. More generally, any cross section shape defined by $\eta(x)$ is allowed, but the hull shape must of course be similar for all stations, according to Eq. (74). The connection betweeen the shape function $\eta(x)$ and stream function $\psi(x)$ may be obtained from Eq. (27), and we have

$$\psi(x) = 2\lambda U x\eta(x) - \lambda U(\gamma+2)\int_0^x \eta(\xi)\, d\xi \tag{75}$$

A physical justification of this similarity solution may be attempted as follows. At these high Froude numbers we are concerned only with the *diverging* part of the ship wave pattern near the ship's track, since the *transverse* wavelength $2\pi U^2/g$ far exceeds the ship length. The diverging waves are short in wavelength even for vanishing gravity,[21] and in fact their crests asymptote to the axis $x=0$ according to the parabolic law, $x \sim s^2$ Thus the growth of the waterplane [Eq. (57)] precisely matches the spreading of the diverging waves.

Given this physical picture we may speculate on the character of the solution, especially near the leading edges, for other waterplanes. For example, if the waterplane is *less highly cusped* than Eq. (57); i.e., $n<2$ in Eq. (54), the rate of spreading of waves exceeds the rate of growth of waterplane, and at some station the diverging waves must emerge from beneath the hull, changing fundamentally the character of the leading edge singularity and hence the spray sheet.

VI. Numerical Procedure

In this section we discuss a procedure for numerical solution of the integral equation (37). The program used is quite unsophisticated, and further work is needed to develop more efficient programs. However, the accuracy attainable with the present method is satisfactory for some purposes.

The only numerical difficulty in solving Eq. (37) is with the double-integral term. Routines for efficiently inverting finite Hilbert transforms are easy to construct, so that the first term on the right of Eq. (37) gives no trouble. Notice that the double-integral term contains all "time"-history effects; that is, it and only it introduces an influence of previous stations $\sigma<s$ on the pressure at the current station s. In this connection it is important to note that the kernel K_σ *vanishes* at the current station, i.e., when $\sigma=s$.

We make use of this property in a "time"-stepping procedure, by first using the ordinary trapezoidal rule on the σ-integration. Having chosen a station spacing Δs, we write

$$Q_n(x) = Q(x, n\Delta s) \tag{76}$$

$$\psi_n(x) = \psi(x, n\Delta s) \tag{77}$$

$$b_b = b(n\Delta s) \tag{78}$$

and approximate

$$\rho U\psi_n(x) = \mathcal{K}_{b_n} Q_n(x) - \Delta s\sum_{k=1}^{n-1}\int_{-b_k}^{b_k} d\xi\, Q_k(\xi)\, K_\sigma(x-\xi, (n-k)\Delta s) \tag{79}$$

Equation (79) can be written in the form of a recursive algorithm for Q_n, namely

$$Q_n(x) = \mathcal{K}_{b_n}^{-1} R_n(x) \tag{80}$$

[¶] Remarkably, the special case $\gamma=2$ allows similarity solutions with the nonlinear free surface condition, Eq. (6).

where

$$R_n(x) = \rho U \psi_n(x) + \Delta s \sum_{k=1}^{n-1} \int_{-b_k}^{b_k} d\xi \; Q_k(\xi) \; K_o(x-\xi, (n-k)\Delta s) \qquad (81)$$

Note that R_n is determined from the known quantity $\psi_n(x)$, together with all $Q_k(x)$, $k=1,2,\ldots n-1$, which are known at the nth step.

The next problem is evaluation of the ξ-integral in Eq. (81). We use a very crude estimate, in which $Q_k(\xi)$ is taken as a constant, say Q_{jk}, on each of $2M$ segments, $j=\pm 1, \pm 2, \ldots \pm M$, where the jth segment is defined by

$$\xi_{j-1} < \xi < \xi_j = b_k \sin(j\pi/2M) \qquad (82)$$

Note that the same number $2M$ of x-wise segments is used at every station s, the segment size increasing with waterplane width $2b_k$.

Using the formula of Eq. (38) for K_o and integrating explicitly with respect to ξ,

$$R_n(x) = \rho U \psi_n(x) - \frac{2}{\pi} \sum_{k=i}^{n-1} \frac{1}{n-k} \sum_{\substack{j=-M \\ j\neq 0}}^{M} Q_{jk} \left[F'(\omega) \right]_{\xi=\xi_{j-1}}^{\xi=\xi_j} \qquad (83)$$

with

$$\omega^2 = \frac{g(\Delta s)^2 (n-k)^2}{4U^2 |x-\xi|} \qquad (84)$$

We now evaluate Eq.(83) at a point $x=x_i$, which is approximately the mid-point of the ith segment, namely,

$$x_i = b_k \sin[(i-\tfrac{1}{2})\pi/2M] \qquad (85)$$

obtaining a set of values $R_{in}=R_n(x_i)$. Finally, a numerical inverse Hilbert transform, essentially evaluating an expression like Eq. (42) by the midpoint rule (after removing the Cauchy singularity), provides a corresponding set of values of $Q_{in}=Q_n(x_i)$. We now proceed to station $n+1$, etc. Note that no matrix manipulation (especially no inversion) is ever required in this method.

Difficulties arise because of the highly-singular nature of the kernel near $\xi=x$, as indicated by Eq. (31). Of course we never evaluate exactly *at* this point, and in obtaining Eq. (83) from Eq. (81) have integrated analytically through this singularity. Nevertheless, there is bound to be trouble in Eq. (83) due to large values of ω whenever the point of evaluation $x=x_i$ at some station s is close to an *end* point $\xi=\xi_j$ of any segment at a previous station σ. Physically, each end point of a segment looks like an isolated singularity, which leaves its own "trail" in the form of wildly oscillating waves.[21] A better numerical method could be one in which the step-function character of $Q_k(\xi)$ with ξ was replaced by a smoother variation, thereby moderating the apparent singularity.

This problem manifests itself in the form of apparently-random small fluctuations of $R_n(x)$ as a function of x, superposed upon a "believable" smooth curve. It is cured in a not altogether satisfactory manner by two separate smoothing procedures. In the first place, we test each end point ξ_j while evaluating Eq. (83) to ensure it is not too close to the current evaluation point x_i. If it is as close to x_i as 20% of the ith segment size, we shift x_i (staying within the i-th segment) by that 20% amount. Secondly, after complete evaluation of the $R_n(x_i)$, we smooth by replacing $R_n(x_i)$ by the mean of itself and the linear interpolate between $R_n(x_{i-1})$ and $R_n(x_{i+1})$.

The particular trigonometric lateral spacing [Eq.(82)] was chosen to provide a sufficient density of segments near the edges to counter the rapid (square-root) drop to zero of Q. In fact, explicit use is made of the nature of this spacing to make the inverse Hilbert transform most efficient, and for example the program reproduces *exactly* the result [Eq. (43)] for flat plates at infinite Froude number. However, this decision was made before the singular character of Q near the center plane was discovered. Actually the investigation of Sec. IV was only carried out as a result of the appearance of the numerical results, and in retrospect it would appear that a greater density of points near the center plane would have been desirable.

VII. Discussion of Computed Results

Figure 2 shows results for $Q/\rho U^2 \alpha b(s)$ plotted against $x=x/b(s)$ at various stations s, for the case of a flat plate with the cusped parabolic waterplane of Eq. (57). This is the case in which a similarity solution exists, such that the quantity plotted should be independent of s. The results shown are for $M=20$ and a maximum value of $n=20$, with the speed chosen so $\nu=1.25$. For example, with a length/beam ratio of 5.0, this would correspond to a conventional Froude number $F=2.0$.

Observe that at this fairly-high Froude number, a similarity profile is reasonably well achieved by about the mid-section of the ship. In fact, departure from similarity very near the bow is inevitable, since the program starts with $R_1(x)=0$ in Eq. (80). That is, at the very first station $n=1$ there is an apparent infinite-Froude-number or zero-gravity solution, irrespective of the actual Froude number. This is shown as the $s=0$ curve in Fig. 2, and is simply the elliptic loading of Eq. (43). The behavior for the first few stations is quite erratic, but the oscillations apparently die out as s increases.

If we now vary ν, i.e., vary the Froude number, we obtain the family of similarity profiles shown in Fig. 3. These are essentially plots of $Q(x)$, as in Eq. (70) with $\gamma=1$. However, they are actually obtained as in Fig. 2 from the general program at $s/L=1.0$. Similarity is harder to achieve

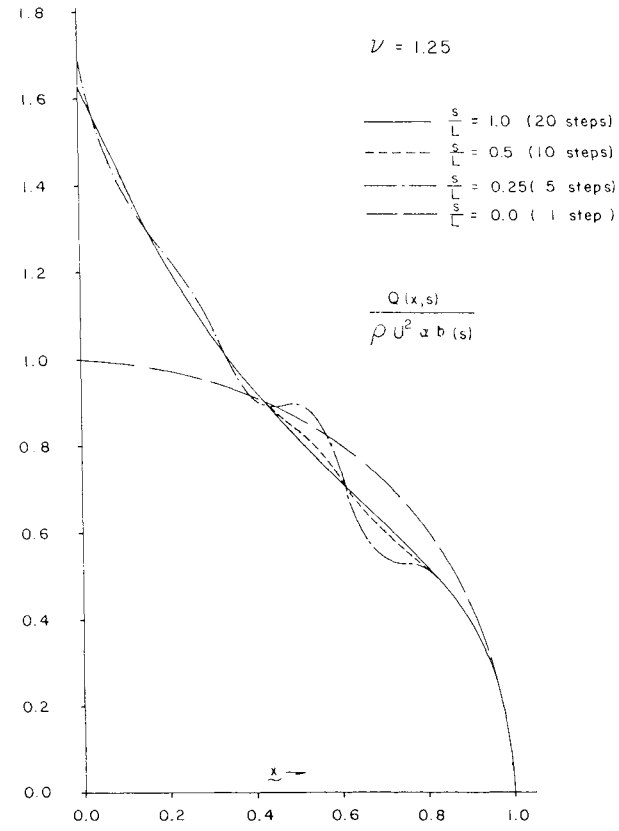

Fig. 2 Similarity check for cusped waterplane. Scaled loading distribution at various stations, for fixed $v=gL^2/U^2B$.

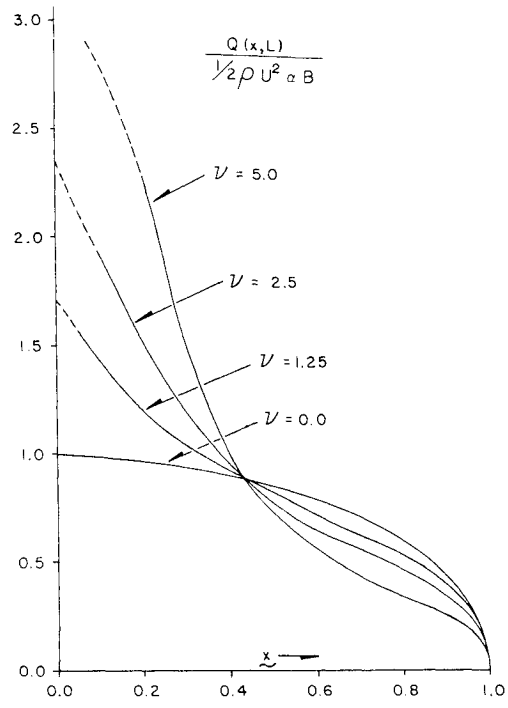

Fig. 3 Trailing edge loading distribution for cusped waterplane at various values of $v = gL^2/U^2B$.

numerically as ν increases, i.e., as the effect of gravity increases, especially near the center plane. The curves are dashed wherever an uncertainty of more than ~5% exists, and discontinued altogether as soon as the uncertainty reaches ~10%.

Corresponding curves of the actual pressure ***P(x)*** could be obtained from Eq. (71), but the necessary numerical differentiation would reduce the accuracy of the results unacceptably. However, it is clear that the general character is of a sharp but finite pressure peak at the center plane, with a pressure minimum about halfway out, followed by an infinite positive-amplitude (inverse-square-root) peak at the edge $x=1$. This infinity corresponds to the leading-edge spray sheet.

Figure 4 shows the loading Q at the trailing edge $s/L=1.0$ for the case of a *triangular* waterplane, i.e., for a delta wing, at various values of ν. The results are analogous to those of Fig. 3, but the profiles are no longer self-similar with respect to s. On the contrary, Fig. 4 has an alternative interpretation as a plot of scaled loadings at various stations s for a *fixed* value of ν. For example, at $\nu=2.5$ the loading at the *midsection, $s/L=0.5$*, is precisely *half* of the result shown in Fig. 3 for the trailing-edge loading at $\nu=1.25$.

In both Figs. 3 and 4 the center-plane singularity suggested by the analysis of Sec. IV is qualitatively evident. Unfortunately, program accuracy in this region is, not surprisingly, least satisfactory, so that we are not able to verify the differences in the actual degree of singularity, as indicated by Eq. (55).

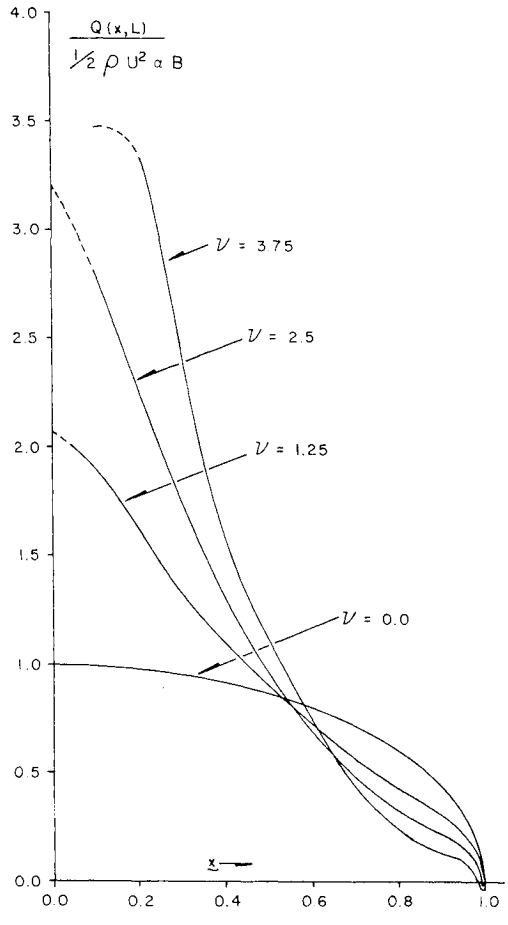

Fig. 4 Trailing edge loading distribution for triangular (delta wing) waterplane, at various values of $v = gL^2/U^2B$.

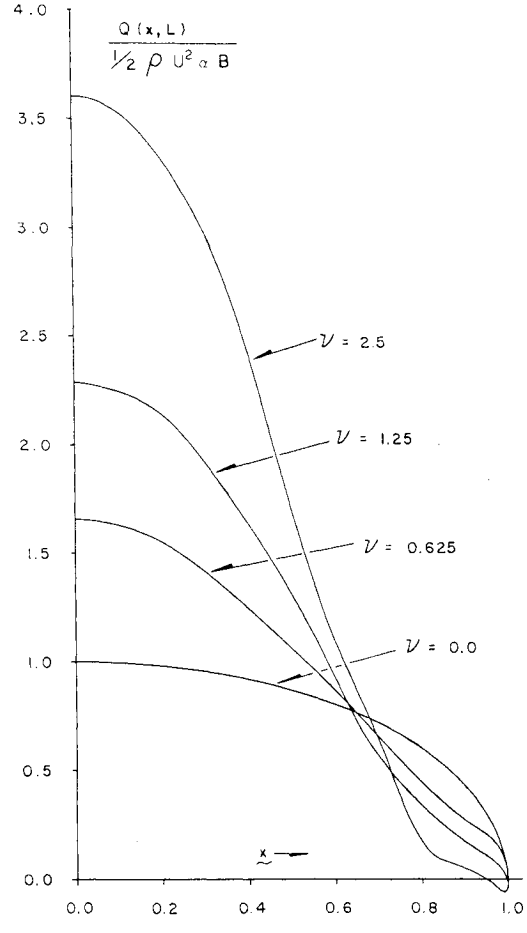

Fig. 5 Trailing edge loading distribution for blunt waterplane at various values of $v = gL^2/U^2B$.

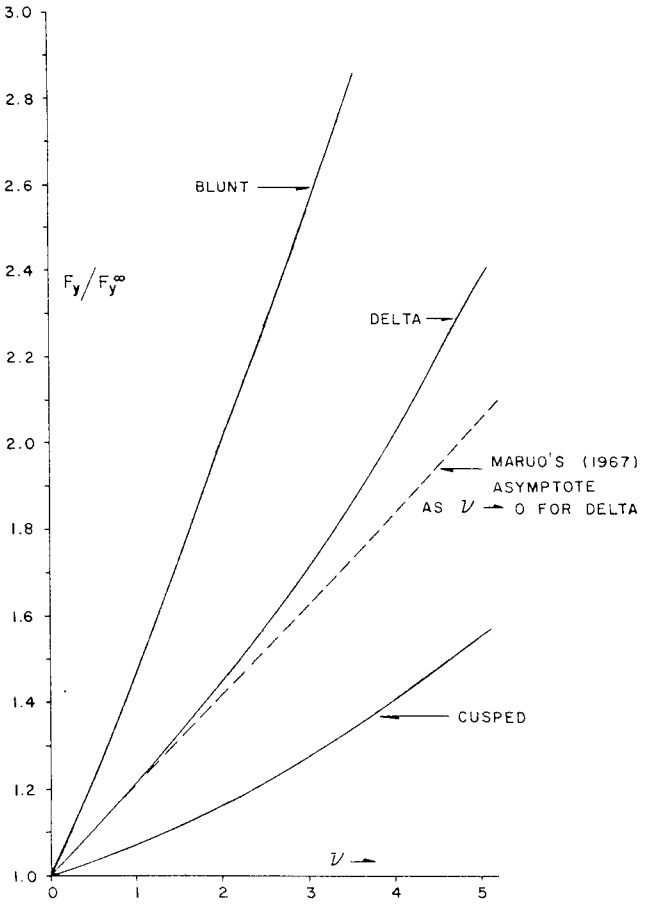

Fig. 6 Lift of various flat plates, scaled with respect to the zero-gravity limit, and plotted against $\nu = gL^2/U^2B$.

Perhaps a more significant difference betweeen Figs. 3 and 4 is in the strength of the pressure singularity at the *edge* $x=1$, which appears approximately invariant with ν for the similarity profiles of Fig. 3. In the case of the delta wing, however, there appears to be a real *weakening* of the pressure singularity as ν increases, or as we move from bow to stern at fixed ν. In fact for all $\nu > 2.1$ the computer program predicts *small negative* loadings very near to $x=1$. Since this implies a negative infinity in the pressure, it is not a physically-acceptable result. Unfortunately it is hard with the present crude program to tell whether there are genuine theoretical predictions, or numerical errors. However, the fact remains that no such negative values are ever obtained in the similarity case of Fig. 3.

This effect is anticipated by the discussion at the end of Sec. 5, and can be illustrated better by use of the *even-blunter* waterplane $n=1/2$ in Eq. (54), i.e., one which is parabolic in s against x. Figure 5 shows loadings for this case. There is now no doubt from the computer output that for $\nu > 1.1$ the predicted edge loading is *negative*. What actually happens here is not clear; what is clear, however, is that the present theory is no longer valid. Note also from Fig. 5 that for this blunt body, the center-plane singularity has almost disappeared and the pressure gradient now appears to vanish at $x=0$, as predicted in Sec. IV.

Figure 6 shows the variation with ν of the lift force F_y, computed according to Eq. (33) and scaled with respect to the infinite Froude-number (i.e., $\nu=0$) value

$$F_y^\infty = \tfrac{1}{2}\pi\rho U^2 \alpha [b(L)]^2 \tag{86}$$

Results for all three waterplanes discussed above are shown. For the triangular case only, comparison may be made with Maruo's very-high-Froude-number approximation[1]

$$F_y/F_y^\infty = 1 + 0.211\,\nu \tag{87}$$

a straight line which clearly gives the correct asymptotic behavior for small ν.

References

[1]Maruo, H., "High- and Low-Aspect Ratio Approximation of Planing Surfaces," *Schiffstechnik,* Vol. 72, 1967, pp. 57-64.

[2]Michell, J.H., "The Wave Resistance of a Ship," *Philosophical Magazine,* Ser.5 Vol. 45, 1898, pp. 106-123.

[3]Ogilvie, T.F., "Non-Linear High-Froude Number Free-Surface Problems," *Journal of Engineering Mathematics,* Vol. 1, 1967, pp. 215-235.

[4]Wang, D.P. and Rispin, P., "Three-Dimensional Planing at High Froude Number," *Journal of Ship Research,* Vol. 15, 1971, pp. 221-230.

[5]Gilbarg, D., "Jets and Cavities," *Handbuch der Physik,* Vol. 9, Springer, Berlin, 1960.

[6]Tuck, E.O. and Von Kerczek, C., "Streamlines and Pressure Distribution on Arbitrary Ship Hulls at Zero Froude Number," *Journal of Ship Research,* Vol. 12, 1968, pp. 231-236.

[7]Acosta, A.J. and Delong, R.K., "Experimental Investigation of Non-Steady Forces on Hydrofoils Oscillating in Heave," presented at the IUTAM Symposium on Non-Steady Flow of Water at High Speeds, Leningrad, 1971.

[8]Tulin, M.P., "The Theory of Slender Surfaces Planing at High Speeds," *Schiffstechnik,* Vol. 4, 1956, pp. 125-133.

[9]Monacella, V.J. and Newman, J.N., "The Pressure on the Sea Bottom Due to a Moving Pressure Distribution," NSRDC Rept. 2308, 1967, Dept. of the Navy, Washington, D.C.

[10]Gadd, G., "A Method for Calculating the Flow Over Ship Hulls," *Transactions of the RINA,* Vol. 112, 1970, page 335.

[11]Van Oortmerssen, G., "Some Aspects of Large Offshore Structures,"presented at the 9th Symposium on Naval Hydrodynamics, Paris, 1972.

[12]Oertel, R., "The Steady Motion of a Flat Ship, with an Investigation of the Flow near the Bow and Stern," Ph.D. Thesis, Applied Mathematics Dept., Univ. of Adelaide, Adelaide, Australia, 1974.

[13]Havelock, T.H., "The Theory of Wave Resistance," *Proceedings of the Royal Society of London,* Ser. A, Vol. 138, 1932, pp. 339-348.

[14]Rogallo, R.S., "A Trailing-Edge Correction for Subsonic Slender-Wing Theory," Ph.D. Thesis, Dept. of Aeronautics and Astronautics, Stanford University, 1969.

[15]Tuck, E.O., "A Systematic Asymptotic Expansion Procedure for Slender Ships," *Journal of Ship Research,* Vol. 8, 1964, pp. 15-23.

[16]Abramowitz, M. and Stegun, L.A., eds., "Handbook of Mathematical Functions," National Bureau of Standards, Washington, D.C., 1964, p. 300.

[17]Lamb, H., *Hydrodynamics,* 6th ed., Cambridge and Dover, London, 1932, p. 384.

[18]Cummins, W.E., "The Wave Resistance of a Floating Slender Body," Ph.D. Thesis, American University, 1956.

[19]Tricomi, F.G., *Integral Equations,* Interscience, New York, 1957, p. 174.

[20]Newman, J.N. and Wu, T.Y-T., "A Generalized Slender-Body Theory for Fish-Like Forms," *Journal of Fluid Mechanics,* Vol.57, 1973, pp. 673-693.

[21]Ursell, F., "On Kelvin's Ship Wave Pattern, "*Journal of Fluid Mechanics,* Vol. 8, 1960, pp. 418-431.

[22]Wehausen, J. V. and Laitone, E. V., "Surface Waves," *Handbook der Physik,* Vol. 9, Springer,Berlin, 1960.